J Low Temp Phys (2016) 185:324–338
DOI 10.1007/s10909-016-1638-1

# Instability on the Free Surface of Superfluid He-II Induced by a Steady Heat Flow in Bulk

**I. A. Remizov**[1] · **A. A. Levchenko**[1] · **L. P. Mezhov-Deglin**[1]

Received: 29 February 2016 / Accepted: 2 June 2016 / Published online: 21 June 2016


**Abstract** We report observations of the onset of irregular motion on a free surface of superfluid He-II induced by a quasi-stationary heat flow in a rectangular container. The container open from the top is mounted inside an optical cell partly filled with superfluid He-II. Three holes in the container walls provide free circulation of the normal and superfluid components inside and outside the container. The results of measurements are discussed in terms of the Korshunov theory (Eurphys Lett 16:673, 1991; JETP Lett 75:423, 2002) of the Kelvin–Helmholtz instability on an initially flat He-II surface induced by a relative motion of superfluid and normal components of the liquid along the surface when the counterflow velocity exceeds the threshold value. The experimental data are qualitatively consistent with the theoretical predictions (Korshunov in JETP Lett 75:423, 2002) taking into account the finite viscosity of He-II.

**Keywords** Superfluid helium · Heat flow · Counterflow of normal and superfluid components · Surface elevations · Kelvin–Helmholtz instability on a free surface

It is our great honour and a great pleasure to submit our paper to the special issue of JLTP dedicated to Prof. Horst Meyer. One of us (L.P. M-D.) has known him since the beginning of 1970s , and we had multiple opportunities to converse with him on a number of topics like quantum diffusion of point defects in quantum crystals, gravity-driven convection in near-critical fluids with different heating, and many others, at a number of low temperature conferences in USA, Russia, Ukraine and Kazakhstan. We also had relatively frequent communications through long years, which sometimes included his visits to the last three countries, and these communications are our unforgettable remembrance.

✉ L. P. Mezhov-Deglin
mezhov@issp.ac.ru

[1] Institute of Solid State Physics Russian Academy of Sciences Chernogolovka, Moscow District, 2 Academician Ossipyan str., Chernogolovka, Russia 142432

## 1 Introduction

In this paper, we present the results of our recent investigations of a dynamical instability on the surface of superfluid He-II induced by the relative motion (counterflow) of normal and superfluid components caused by a stationary heat flow within the liquid. The theory of this phenomenon was first considered in details by Korshunov [1,2] and later on by Andersson et al. [3] who investigated the instability on the superfluid neutron surface on neutron stars. This instability is similar to the well-known two-flow instability on the boundary between two ordinary immiscible liquids or dense gases (Landau, [4]), on boundaries between two phases of superfluid $^3$He (Blaauwgeers et al. [5], Volovik [6]) or on the atomically rough interface between solid and liquid helium (Kagan [7]), and is known to operate in plasmas, cosmic objects, etc. It is analogous to the Kelvin–Helmholtz (KH) instability, with the difference being that both sliding liquids (normal and superfluid components) are located on the same side of the interface. The instability sets in once the velocity of counterflow reaches a threshold level. The theoretical analysis is based on the two-fluid equations of the standard Landau model for superfluid helium [4]. Volovik [6], and later Korshunov [2] and Andersson [3], showed that taking into account the inner viscosity of He-II shifts the point of instability from the well-known classical threshold [4] to another value. However, all the above theories neglect a strong nonlinearity of the surface waves and waves of second sound in He-II. Moreover, these theories disregard a possible development of the vortex turbulence in the bulk of He-II at high-flow velocities (large heat fluxes). As a result a considerable divergence in theoretical values of the threshold heat fluxes [2,3] from the experimental data (see Olsen et al. [8–10] and Abdurakhimov et al. [11]) are observed.

The two-flow instability in superfluid He-II due to relative motion of the superfluid and normal components is perhaps one of the simplest and clearest cases. A permanent counterflow of normal and superfluid components within the liquid can be maintained by applying a stationary heat flow to He-II by a resistive heater. Investigations of the corrugation instability on the He-II-free surface in the presence of an equilibrium counterflow could provide insight into this phenomenon and make theoretical predictions more precise.

## 2 Theoretical Background: Corrugation Instability on the Free He-II Surface Induced by an Equilibrium Counterflow within the Superfluid

Note that in this study the total mass flow in the liquid in a locked container of finite sizes is absent $j = \rho_n v_n + \rho_s v_s = 0$, and the counterflow velocity $w$ inside He-II is defined by the density of heat flow $Q/\Sigma$ delivered into the liquid by a resistive heater. It is supposed that the heater surface area $\Sigma$ coincides with the cross-section of the rectangular container, and $Q$ is the heat power delivered by the heater into He-II. So the normal and superfluid components are moving within the liquid parallel to the He-II-free flat surface, and the absolute value of the counterflow is

$$|w| = |v_n| + |v_s| = |v_n|\rho/\rho_s \tag{1}$$

Here $\rho_n$, $v_n$ and $\rho_s$, $v_s$ are the density and velocity of normal and superfluid components, and the total density $\rho = \rho_n + \rho_s$. Following Landau [4], the velocity of the normal component moving in He-II from the heater is

$$v_n = (Q/\Sigma)/(\rho ST) \tag{2}$$

where $S$ is the entropy per unit mass. The relative motion of the normal and superfluid components within the superfluid should result in an additional internal pressure

$$\Delta p = 1/2(\rho_n v_n^2 + \rho_s v_s^2) \tag{3}$$

The additional internal pressure on the liquid surface created by switching on the heater could be written as

$$\Delta p = 1/2(\rho/\rho_s)(Q/\Sigma\rho ST)^2 \tag{4}$$

At the heat flow above a certain threshold value $(Q/\Sigma)_{\text{thr}}$, the initially flat-free surface of superfluid $^4$He loses stability because of strong surface deformation caused by the relative motion of normal and superfluid components.

In the work [1], the author neglected the influence of viscosity within the superfluid and supposed the viscosity coefficient to be zero $\eta = 0$ by conditions. In the frame of the nondissipative two-fluid description and supposing the mass velocity within the liquid in a container equals to zero, the dispersion relation could be written as

$$\omega^2 = gk + (\sigma/\rho)k^3 - (v_n k)^2(\rho_n/\rho_s) \tag{5}$$

Here $\sigma$ is the surface tension and $k$ is the wave vector of the surface wave. It is evident from (5) that the frequency of the surface waves should decrease (softening of the dispersion law) with increasing $v_n$ (or the heat flux density). And at $Q$ large enough, when the right-hand side of equation (5) becomes negative, the surface becomes unstable. The corrugation instability of the free surface starts developing at a critical wave vector

$$k_c = (\rho g/\sigma)^{1/2} \tag{6}$$

which is equal to $k_c = 21\ \text{cm}^{-1}$ at $T = 1.8$ K. Note that in the temperature range $T = 1.2$–$2$ K we can disregard the temperature dependence of density and surface tension, and take $\rho = 0.14\ \text{g/cm}^3$ and $\sigma = 0.3$ dyn/cm [12], so that $k_c$ also becomes temperature–independent, at least to the first approximation.

For convenience, we can re-write Eq. (5) in a slightly different form

$$\omega^2 = gk + (\sigma/\rho)k^3 - (wk)^2(\rho_n\rho_s/\rho^2) \tag{7}$$

The form of Eqs. (5–7) shows that the roots with positive and negative imaginary parts (the former correspond to growing corrugation) exist only if the absolute value of $w$ exceeds certain $w_{c0}$ defined by

$$w_{c0}^2 = 2(\rho^3 g\sigma)^{1/2}/(\rho_n\rho_s) \tag{8}$$

with the instability taking place at the same wave vector $k_c = (\rho g/\sigma)^{1/2}$ (6). We denote this critical velocity as $w_{c0}$ to emphasize that it corresponds to the limit of zero viscosity, $\eta = 0$

For any finite $\eta > 0$, the dispersion relations (5, 7) should be modified to take into account the finite dissipation in the bulk (in accordance with Eq. (12) in [2]). The dispersion relation (12) for viscous superfluid He-II includes real and imaginary components. As shown in [2], one of the roots of the modified dispersion equation crosses the real axis already when the sum

$$S(k) = gk + (\sigma\rho)k^3 - (wk)^2(\rho_s/\rho) \tag{9}$$

becomes equal to zero. Then the reconsidered value of the critical velocity $w_c$ is given by

$$w_c^2 = 2(\rho g/\sigma)^{1/2}/\rho_s = w_{c0}^2(\rho_n/\rho) \tag{10}$$

Note that this threshold velocity $w_c$ is lower than $w_{c0}$ by a factor of $(\rho/\rho_n)^{1/2}$ though the wave vector corresponding to the onset of instability remains equal to $k_c$ (6). Keeping in mind that $v_n = (Q/\Sigma)/\rho ST$ and the mass flow within the liquid in the container is equal to zero, the value of the threshold heat flux density $(Q/\Sigma)_{\text{thr}}$ necessary for the development of an instability on the free He-II surface can be written as

$$(Q/\Sigma)_{\text{thr}} \geq ST(2k_c\sigma\rho_s) \tag{11}$$

where $S$ and $\rho_s$ depend strongly on temperature, while the surface tension $\sigma$, and the critical wave vector $k_c$ are weakly dependent on T in the range $T$=1.2–2.0 K. Using the values of $\rho_n$, $\rho_s$, specific entropy and surface tension given in Ref. [12], we estimated that the value of threshold heat flux should be $(Q/\Sigma)_{\text{thr}} \geq 1.8$ W/cm$^2$ at $T$=2 K, $\geq$0.6 W/cm$^2$ at $T$=1.8 K and $\geq$0.15 W/cm$^2$ at $T$=1.3 K. For comparison, in the experiments [8–10] first reporting the development of the surface instability induced by the heat flow in He-II, the internal pressure was mainly created by the standing second sound waves. According to our estimations the density of an alternating heat flow in the liquid layer next to the heater surface was as high as $\geq$0.25 W/cm$^2$ at $T$=1.8 K.

## 3 Experimental Observations of an Instability on the Free Surface of He-II Induced by a Stationary Heat Flow

### 3.1 Preliminary Study of the Surface Instability Induced by the Heat Flow Within the Superfluid He-II in the Container with Impenetrable Lateral Walls

In the earlier our work [11], we attempted to reproduce the results of observation of the surface patterns described in [8–10], but under different boundary conditions. It was found in [8–10] that the standing second sound waves excited by a wire heater in a cylindrical resonator filled in part with superfluid He-II could generate surface waves, and the development of instability can be observed on the free surface with

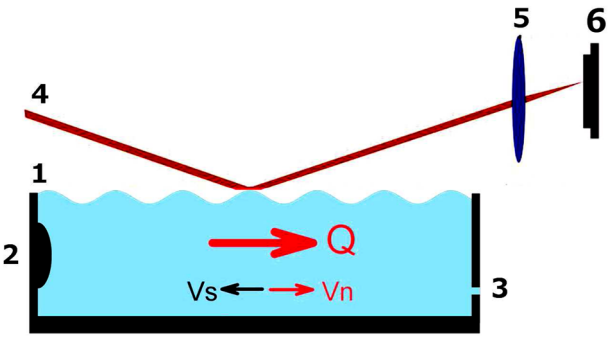


**Fig. 1** Scheme of the experiment: 1—the rectangular container; 2—the resistive heater; 3—holes in the lateral walls (used in the main experiments, only); 4—the laser beam; 5—the lens and 6—the photodetector (Color figure online)

an increasing heat flux density. The observed surface deformations were mainly connected with the steady component of the additional pressure (3) created by the standing wave below the surface. The specific characteristics of the second sound - surface wave interaction were studied by Khalatnikov et al. [13–15]. Direct transformation of the low-frequency (less than a few kHz) second sound wave into a surface wave in the gravity-capillary range of frequencies is impossible because of a strong difference in the dispersion laws: the curves $\omega(k)$ can intersect only at high frequencies above $10^8$ Hz. Therefore, the surface waves could be generated by the standing second sound waves due to any parametric excitations.

At small heat fluxes, the spatially periodic surface structures were immobile, and the height of the surface wave was proportional to the heat flux. With an increase of the excitation level, the deviation from the sinusoidal shape of surface waves occurs at critical heat fluxes corresponding to the critical slope of the surface elevations 0.03–0.04. The growth of the heat flux to a certain critical value gave rise to an abrupt transition to a new wave structure with a doubled wave number and of much larger amplitudes (a variety of harmonic oscillations occurred). And at the largest heat fluxes (above the threshold value), chaotic oscillations occurred. It was suggested in [10] that the observed phenomena might be considered as a manifestation of a nonequilibrium phase transition. So, the main aim of our preliminary study was to try to reproduce those observations, qualitatively at least, but under differing boundary conditions.

The scheme of our measurements is shown in Fig. 1. The rectangular container 1 open from above with impenetrable (in the preliminary study) side walls was surrounded from outside by a bath of He-II (not shown in the figure). The container of $30 \times 24$ mm inner sizes and 5 mm deep was made of the material with low heat conductivity (plexiglass). The container was mounted inside an optical cell (not shown in the scheme) suspended at a copper rod in the high vacuum inside a metal optical cryostat. The copper rod served as the thermal link connecting the optical cell with the helium vessel of the cryostat. The temperature of the liquid in the vessel could be lowered to 1.3 K by pumping He vapours from the vessel. The level of He-II in the locked optical cell coincided with the upper edge of the container, so the mass flow

inside the container was zero. The heat flux in the container was radiated by a thin metal film 2 with the surface $\Sigma = 1.2$ cm$^2$ mounted on a lateral wall of the container.

The surface oscillations were monitored by recording the power variation of the reflected laser beam 4 from the liquid surface in the same manner as in [16,17]. The beam was incident on the surface at a small grazing angle of 0.1 rad. The maximum wave amplitude on the liquid surface before transition to a corrugated state did not exceed typically 0.2 mm. The beam reflected from the vibrating surface was focused onto the photodetector 6 by the outer lens 5. The voltage on the photodetector was proportional to the power of the reflected laser beam. The variable component of the laser beam power $P(t)$ was recorded by a computer through a high-speed 24-bit A/D converter, with a digitizing frequency of 102.4 kHz for several seconds. To elucidate the frequency distribution in the spectra of surface oscillations $P(t)$, we analysed the frequency spectrum $P_\omega$ obtained by the time Fourier transform of the recorded $P(t)$-dependence ($P_\omega$ denotes the absolute value of the Fourier transform). The power variation $P(t)$ was determined by the relation between the sizes of the light spot, the wavelength of the surface wave $\lambda$ and also by the inclination of the liquid surface. If the wavelength of the ripples is much greater than the axis of the light spot (low-frequency approximation, gravitational waves), the beam can be considered to be thin. Due to the small sizes of the grazing angle and the surface deviation from equilibrium, the power variation of the thin laser beam is proportional to the deviation angle, $P = \phi(t)$. The angle $\phi$ can be written as the ratio of the wave amplitude $\eta$ to its length $\lambda$.

The correlation function of surface elevation in the low-frequency limit (gravitational waves, the frequency $f \ll 30$ Hz, the narrow beam approximation) can be written in the frequency representation as follows:

$I_\omega = |\eta_\omega|^2 \sim P_\omega^2 \omega^{-4/3}$,

where $P_\omega^2$ is the frequency distribution of squares of the Fourier component for the experimentally measured time dependence of the reflected beam power $P(t)$. In the opposite case $f \gg 30$ Hz (capillary waves, high-frequency approximation—a wide beam), the registered power of the reflected beam is determined through the value of the surface inclination averaged over the area of the light spot. The calculations show that the change in the reflected beam power as a whole is proportional to $P_\omega \sim \lambda \phi_\omega$—the product of the amplitude of angle variation $\phi$ by the wavelength $\lambda$. This gives the relation $I_\omega \sim P_\omega^2$ in the high-frequency limit. The transition from the low to high-frequency limit (gravity-capillary waves) occurs in the frequency range near 20–40 Hz. The appropriate experimental results demonstrating the evolution of the surface oscillations spectrum in the rectangular container at $T = 1.8$ K with an increase the dc or ac heat flux density are shown in [11] in Figs. 13–16. In agreement with the results of [8–10] it was established that the occurrence of surface oscillations was mainly determined by the total power of heat flow radiated by the heater. The experimental results described in Refs. [8–10] and [11] clearly showed that the presence of a uniform steady heat flow component is crucial for the formation of the surface instability.

The geometry of the experiments (boundary conditions) and the direction of the heat flow in [11] and [8–10] strongly differ from each other and from that considered in the theory [1,2]—a uniform flow of the normal component parallel to the free surface of superfluid He-II. In [11], the heat flux delivered by the heater 2 to the container 1 could be transferred to the outside helium bath in part via the helium film covering the

container walls and via re-condensation of He vapours from the surface of liquid in the container on the surface of He-II surrounding the container in the locked optical cell (the vapour pressure in the optical cell did not change, so it worked as a condensation pump). Therefore it was difficult to expect that the numerical estimates of the critical heat fluxes in those measurements would coincide with each other or with the theory [2]. It is of importance to emphasize the qualitative agreement between the results of observations in the works [11] and [8–10] which can be presented as (a) at relatively low alternating heat fluxes the spatially periodic surface structures were immobile, whereas (b) at higher excitations a variety of harmonics was observed on the spatially immobile surface and (c) at large heat fluxes above a certain threshold value the chaotic oscillations on the surface occurred, both spatially and temporally immobile.

It was specially stretched in [11] that at small total heat fluxes (be it dc or ac heat fluxes from the heater), for example, at $Q/\Sigma < 6 \times 10^{-4}$ W/cm$^2$ at $T = 1.8$ K, switching on the heater did not practically affect the character of low-frequency surface oscillations which were attributed to the noise vibrations of the building. When the amplitude of the heat flux was increased above a certain critical value, the amplitudes and positions of the low-frequency waves and the surface waves connected with the standing second sound considerably changed. This agrees with the softening of the dispersion law as the velocity of the normal component increases in accordance with Eqs. (3) and (5). Because of strong changes in the nature of the surface, oscillations were observed at a heat flow larger than $6 \times 10^{-4}$ W/cm$^2$ (corresponding to the above transitions from case (a) to case (b), the authors of [11] proposed the value $6 \times 10^{-4}$ W/cm$^2$ be considered the critical one. This value is three orders of magnitude less than the value of the threshold heat flux predicted by the theory [2] for the development of the corrugation instability on the surface of He-II, and that of the threshold heat flux estimated from measurements [8–10]. One of the causes of this strong difference could be a significant difference in the boundary conditions. For instance, in [8–10] the steady component of the heat flux was transferred to the outer He-II bath through special holes in the walls of the cylinder resonator. And in [11] the heat flux was mainly transferred by a superfluid helium film covering the protruding parts of the lateral walls. Therefore the velocity of the normal component $v_n$ near the walls was many times higher than in the bulk of the container, and the surface instability might be initially generated near the edge of the walls.

### 3.2 Instability on the Free Surface of He-II Induced by a Stationary Heat Flow Within the Liquid in the Container With Penetrable Lateral Walls

A new series of measurements was carried out in a rectangular container 1 of the linear sizes $24 \times 29$ mm$^2$ and the depth 5 mm similar to the container used in [11], but with lateral walls penetrable for the flow of the normal component (see Fig. 1). For this purpose three holes 2 mm in diameter with centres $\sim$2.5 mm from the bottom of the cell were drilled on each lateral wall (as shown schematically in Fig. 1 ). A low-inertial resistive heater 2 was tightly attached to one of these walls. The heater was made of a standard industrial resistor (MF—0.5 k$\Omega$, 0.25 W) treated specially for the experimental conditions: one half of the long ceramic cylinder 2 mm in diameter

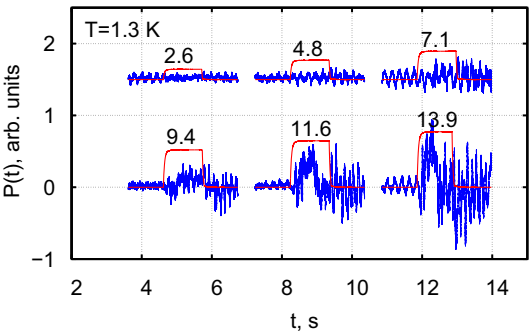


**Fig. 2** Evolution of the shape of surface vibrations $P(t)$ on heating the resistor in He-II by the rectangular pulses (shown by *straight lines*). The bath temperature $T = 1.3$ K. The pulse duration is $\tau = 1$ s. The figures above the pulses indicate the pulse amplitudes $U$ (Color figure online)

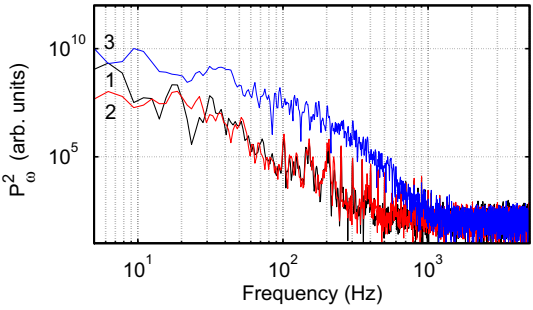


**Fig. 3** The frequency distribution of the power of the surface elevations $P_\omega^2$. The curve *1* corresponds to the background vibrations at zero $U$, recorded before switching on the pulse. The curves *2* and *3* show evolution of the frequency distribution $P_\omega^2$ with increasing the pulse amplitude from $U = 2.6$ to 11.6 V, accordingly. The bath temperature is $T = 1.3$ K (Color figure online)

covered with a thin metal film was deleted, and then the flat back side of the resistor was fixed to the wall, so that it practically overlapped the adjacent holes. The resistor was connected with the outer source of dc voltage. To eliminate the appearance of shock waves (temperature jumps [18,19]) in superfluid He-II on switching on/off the dc voltage, a special high pass filter was installed in the output line of the source, so the transit time at the exit was ∼0.1 s. The heater resistance 2 was R=1 kΩ, the total area of the resistive film $\Sigma \approx 0.3\ cm^2$. Thus, the density of the steady heat flux delivered by the heater to the liquid layer adjacent to the heater surface was

$$Q/\Sigma = U^2/(R\Sigma) \approx 3\times 10^{-3} U^2\ W/cm^2 \tag{12}$$

where U is the voltage applied to the heater.

The stationary heat flow from the heater 2 was moving within the liquid towards the opposite wall of the container and then through the holes 3 in the wall to the outer helium bath surrounding the container. So the boundary conditions for the heat flow in the given experiment were much closer to that assumed in the theory, as compared to previous experiments [8–11]. An example of evolution of the surface vibrations on heating the resistor in He-II by the rectangular electric pulses is shown in Fig. 2. The pulse duration was $\tau = 1$ s, the amplitudes of the voltage pulse $U$ applied to the heater could be varied from 2 to 22 V. The interval between two pulses was over 10 s.

The surface oscillations at zero $U$ (curve 1 in Fig. 3) are connected with the external noises due to low-frequency vibrations of the premises (the background noises).

These vibrations could be considered as a mechanical wide-band noisy excitation in the frequency range 1–10 Hz. Note that in this case the normal and superfluid components are locked together and move under the action of gravity and surface tension forces. The graphs in Fig. 2 show that as $U$ was increased above a certain value (above U = 4.8 V at T = 1.3 K) the amplitudes of the surface vibration were increasing. And above the threshold voltage (above 7 V, on Fig. 2) the surface motion exhibits a chaotic behaviour.

The frequency spectrum of the surface oscillations $P_\omega^2$ shown in Fig. 3 suggests that the growth of the of heat flux density $Q/\Sigma$ from ∼20 to ∼600 mW/cm$^2$ (curve 3 in Fig. 3) leads to an increase of the amplitudes of the surface oscillations in a wide frequency range from ∼1 to ∼600 Hz more than by two orders of magnitude. The strong increase of the amplitude of surface vibrations in a wide frequency range cannot be connected with the film boiling of the liquid near the heater at large heat fluxes. Our direct observation showed that boiling of He-II near the heater surface could occur at heat fluxes above 800 mW/cm$^2$ at $T$ = 1.3 K, growing to 1500 mW/cm$^2$ with temperature rising to 1.95 K. Thus generation of surface vibrations can be attributed to the development of instability on the flat surface of He-II induced by the steady heat flow beneath the surface. In the frequency range $10^2$–$10^3$ Hz, the power spectrum $P_\omega^2$ (Fig. 3) looks similar to the power spectrum of capillary waves in the direct turbulent cascade, which had been observed in experiments [17], devoted to the investigation of turbulent phenomena on the charged surface of He-II.

In accordance with the theoretical predictions [2–4] the growth time of instability should strongly decrease with an enhancement of the heat flow above the threshold. And it tends to infinity as the heat flow approaches the threshold from above. This greatly limits the accuracy of the threshold definition in experiments with rectangular heat pulses. From the graphs in Fig. 2, it can be concluded that at $T$ = 1.3 K, for example, the threshold above which the surface becomes unstable, lies in the range between 100 and 150 mW/cm$^2$. The theory [2] cannot predict the spectrum of spatial and temporal vibrations at the heat flow above the threshold, though the authors [3] associated these surface vibrations with the generation of acoustic excitations.

Fig. 4 displays the changes in surface oscillations at the fixed voltage $U$ = 11.6 V ($Q/\Sigma$ = 400 mW/cm$^2$), while the temperature of He-II increases from 1.33 to 1.95 K. It is seen that the growth time of the instability on the liquid surface at a flux density above the threshold is of the order of several tenths of a second, and this time increases as the liquid temperature rises from 1.33 to 1.60 K. Under the same conditions, the time of vibrations decay can reach several seconds after the heat source is switched off (the two upper curves in Fig. 4). It also follows from the graphs Fig. 4 that at a fixed density of the heat flux $Q/\Sigma$ = 400 mW/cm$^2$ and the pulse duration $\tau$ = 1 s the behaviour of surface motion becomes chaotic at temperatures below 1.6 K. On further heating the liquid above this temperature, no transition to chaotic oscillations was observed. It is also evident that the value of the threshold heat flux increases with increasing the liquid temperature.

We attempted to estimate more precisely the threshold values of the heat flux at different temperatures by using relatively long triangular voltage pulses. Selected results are shown in Fig. 5a–d. Evolution of the surface oscillations with time under the action of heat pulses at temperatures $T$ = 1.3 (a, c) and 1.8 K (b, d) is shown. The

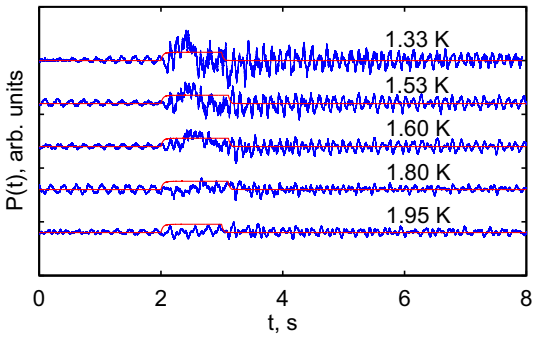


**Fig. 4** Evolution of the shape and amplitudes of the surface vibrations with increasing the temperature of He-II. The pulse duration is $\tau = 1$ s, the pulse amplitude is $U = 11.6$ V (Color figure online)

time durations of the triangular voltage pulses are 5 s (upper row) and 10 s (lower row). The pulse amplitude is 14 V. The frequency distribution in the power spectrum $P_\omega^2$ of the surface oscillations generated by 10 s triangular pulses at $T = 1.3$ and 1.8 K is presented in Fig. 6. The lower dark curves correspond to the background noise oscillations registered within 10 s just before switching on the electrical pulse. The upper curves show the evolution of the frequency distribution under the action of the heat flux. It is seen that as in the case of rectangular heat pulses, the power spectra $P_\omega^2$ shown in Fig. 6 in the frequency range $10^2$–$10^3$ Hz are very similar to the power spectra of the capillary waves in the direct turbulent cascade observed in the study of the turbulent phenomena on the charged surface of He-II [17] under high level of wave excitations.

To determine the moment of an instability generation on the surface of the liquid with increasing the heat flux density, we used the following procedure. Since the results of measurements of the surface oscillations $P(t)$ induced by the heat flow were superimposed by the low-frequency background vibrations in order to determine the instability threshold in experiments with triangular voltage pulses, we first selected the harmonic at the frequency of 20 Hz from the $P(t)$ diagram shown in Fig. 5. Further transformation was to find the envelope of the harmonic. The point of intersection of the envelope with the time axis pointed out the moment of the instability development. This harmonic was selected as a marker of instability because it is present in the Fourier spectrum and lies in the range of transition from gravitational to capillary waves. The harmonic amplitude rapidly grows with time at heat fluxes above the threshold.

An example of the estimation of the threshold voltage $U_{\text{thr}}$ (hence, the threshold density of the heat flux) corresponding to the moment of instability development for two voltage impulses of different durations 5 $s$ and 10 $s$ at the same temperature $T = 1.3$ K is presented in Fig. 7. Dark triangles shown by the straight lines correspond to the voltage pulse applied to the heater; oscillating curves present the amplitude of the surface oscillations rising with time in the $P(t)$ power spectrum shown in Fig. 5a, b at the frequency of $f = \omega/2\pi = 20$ Hz. Vertical dotted lines indicate the moment when the signal envelope intersects the x-axis, and this point is attributed to the initial moment of the instability generation.

The temperature dependence of the threshold heat flux density is shown in Fig.8. Open squares correspond to rectangular pulses, and open circles and crosses corre-

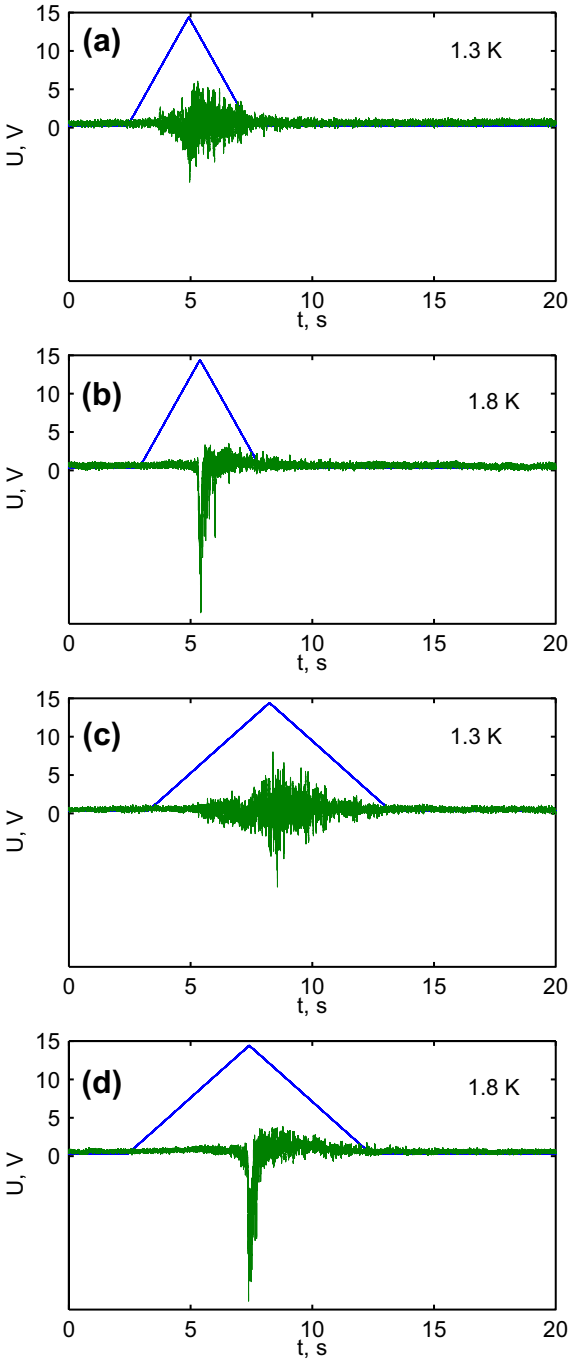


**Fig. 5** Changing the shape and amplitude of the surface oscillations with time under the action of a quasi-stationary heat flow at temperatures $T = 1.3$ (**a**, **c**) and 1.8 K (**b**, **d**) . The time duration of the triangular pulses is 5 s and 10 s. The pulse amplitude U was 14 V (Color figure online)

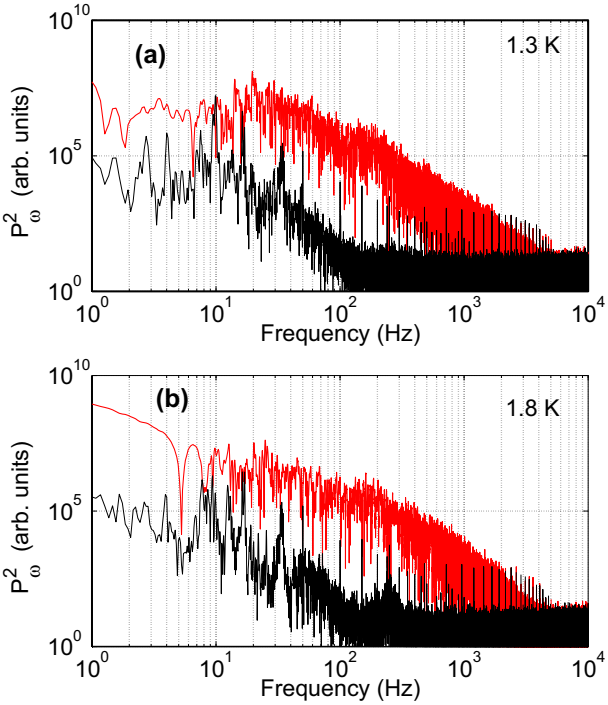


**Fig. 6** Frequency distribution of the power spectrum $P_\omega^2$ of the surface oscillations generated under the action of 10 s triangular pulses at $T = 1.3$ and 1.8 K. *Lower dark curves* correspond to the background noise oscillations registered during 10 s just before switching on the electrical pulse. The *upper curves* show the evolution of the frequency distribution under the action of the heat flux (Color figure online)

spond to measurements on triangular pulses. The solid curve represents the results of the numerical calculations of the threshold flux density $(Q/\Sigma)_{\rm thr}$ made in accordance with the theoretical consideration [2] using the expression (11) from Sect. 2. It seen that the temperature dependence of $(Q/\Sigma)_{\rm thr}$ predicted by the theory agrees fairly well with our experimental data, although the results of numerical calculations shown by points can differ from the theory almost by an order of magnitude.

## 4 Short Discussion

First of all, we should pay attention that for the correct comparison of the experimental data shown by squares, open circles and crosses in Fig. 8 with those predicted by the theory [2] the real profile of the normal component flow below the surface should be taken into consideration [solid curve was calculate by substituting the tabular data from the work by Donnelly [12] into expression (11)]. The values of the threshold heat density estimated from the measurements were related to the heater area $\Sigma = 0.3\,{\rm cm}^2$, which is four times smaller than the cross-section of the container (1.2 $\rm cm^2$). At the same time, the total area of the holes at the opposite lateral wall (position 3 in Fig. 1) is about 0.1 $\rm cm^2$, or 12 times less than the cross-section of the container. Neglecting the

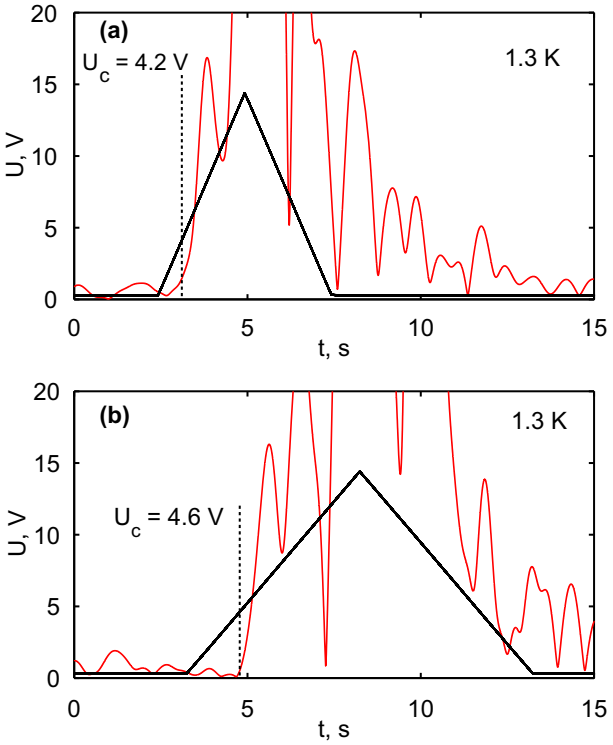


**Fig. 7** An example of estimation of the threshold voltage $U_{\rm thr}$ corresponding to an initial moment of generation of an instability on the surface of He-II at $T = 1.3$ K for two triangular pulses of different durations 5 s (**a**) and 10 s (**b**). Triangular pulses shown by the *straight lines* describe the time evolution of the voltage applied to the heater; oscillating curves show changes over time of the wave amplitude at the selected frequency $f = \omega/2\pi = 20$ Hz in the frequency spectrum $P(t)$ shown in Fig.5. *Vertical dotted lines* show the time, when the signal envelope starts to grow (attributed to the moment of the instability generation) (Color figure online)

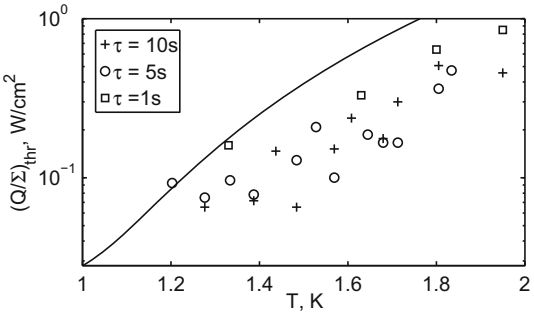


**Fig. 8** Temperature dependence of the threshold heat flux density $(Q/\Sigma)_{\rm thr}$. *Open circles* and *crosses* correspond to the estimations made for triangular pulses of duration of 5 and 10 *s*, and the *open squares* correspond to rectangular pulses. The *solid curve* demonstrates the results of the numerical estimations of $(Q/\Sigma)_{\rm thr}$ calculated in accordance with the results of the theoretical consideration [2]

edge effects, or the boundary conditions near the heater and holes, the effective velocity of the normal component and the proper threshold value of the heat flux density should be divided by 4. In this case, the experimental points shown in Fig. 8 are systematically

overestimated by 4 times. This suggests that we need a better knowledge of the velocity profile inside the liquid, and the influence of this profile on the development of the surface corrugation at large heat fluxes.

Second, in accordance with the predictions by theory [2–4] the growth time of instability at heat fluxes above the threshold should quickly decrease with increasing the flux, but it should tend to infinity as the heat flux drops to $(Q/\Sigma)_{\rm thr}$. This could explain a wide spread of the experimental points shown by the open squares in Fig. 8. In the experiments with rectangular pulses and short triangular pulses, the values of $(Q/\Sigma)_{\rm thr}$ might be overestimated also because the observation time $\tau = 1$ s was not large enough.

Third, in the recent experimental investigations published by A. Makarov, J. Guo et al. [20] the authors studied motion of a cluster of excited He molecules in a long rectangular channel of the cross-section $\Sigma = 0.9\,\mathrm{cm}^2$. The authors [20] observed that in the small heat flux regime $Q/\Sigma \leq 50\,\mathrm{mW/cm}^2$ the flow of normal fluid was laminar, and a profile of the normal fluid flow in a long channel was close to a Poiseuille (parabolic). But, as it was well known from the literature (see references in [20]), above a certain critical heat flux $Q/\Sigma > 50\,\mathrm{mW/cm}^2$ the superflow should become dissipative (quantum turbulence). Observed in this study, flattening of the normal fluid velocity profile as the heat flux was increased above $50\,\mathrm{mW/cm}^2$ had proved that the normal fluid flow also became turbulent. Simultaneous turbulence in both fluids in a counterflow must be different, and it would be a type of turbulence that is new to physics. Thus, it could be of a great interest to expand further the theoretical consideration [2,3] of the Kelvin–Helmholtz instability on the He-II surface taking into account the turbulent flow of normal and superfluid components within the liquid at large heat fluxes.

## 5 Conclusions

In this work, we have investigated the dynamic instability of the free surface of superfluid He-II caused by the relative motion of the superfluid and normal components along the surface. As it was underlined in [2], the value of the instability threshold for finite viscosity is found to be independent of the flow viscosity in He-II, but it is lower than that estimated in the absence of dissipation. It might be of certain interest to extend such a theoretical consideration for a turbulent flow within He-II, taking into account also the strong nonlinearity of the surface waves. These experiments are only a first insight into what promises to be a rich problem area. The future studies must address issues concerning the effects of different dissipation mechanisms, the nonlinear evolution of the instability on the surface and within the liquid. The experiments should also include combination of two different methods of excitation of oscillations on the surface of He-II. For example, excitations by the mechanical vibrations of the container (analogous of the low-frequency noise oscillations, when superfluid He-II is displaced as a whole, and both components are moving in the same direction) in addition to the heat flow within the liquid. These vibrations can serve a seed for the development of surface instability at large heat fluxes [21]. Or the excitation of a charged surface of He-II by external dc and ac electric fields [16,17] (an electric field

is applied in addition to the gravity force and the surface tension), and by the internal pressure arising due to a heat flow below the surface. It is worth noting here that the static electric field can lead to softening of the dispersion law of surface waves and to loss of stability of the charged surface of He-II in large stretching fields; moreover in the study [22] occurrence of macroscopic geysers on a charged surface of He-II was observed at electric fields above some critical value. We hope to investigate these very interesting problems in the near future.

**Acknowledgments** The fruitful discussions with I.M. Khalatnikov, G.V. Kolmakov, E. A. Kuznetsov, V.V. Lebedev and I.V. Kolokolov are gratefully acknowledged. The work was supported by the Russian Science Foundation, Grant No. 14-22-00259.

## References

1. S.E. Korshunov, Europhys. Lett. **16**, 673 (1991)
2. S.E. Korshunov, JETP Lett. **75**, 423 (2002)
3. N. Andersson, G.L. Comer, R. Prix, Mon. Not. R. Astron. Soc. **354**, 101110 (2004)
4. L.D. Landau, E.M. Lifshitz, in Course of Theoretical Physics, Vol. 6: Fluid Mechanics (Pergamon, New York, 1989), Sec. 25, Problem 1; Sec. 62, Problem 3; Sec. 140, Problem 1
5. R. Blaauwgeers, V.B. Eltsov, G. Eska, A.P. Finne, R.P. Haley, M. Krusius, J.J. Ruohio, L. Skrbek, G.E. Volovik, Phys. Rev. Lett. **89**, 155301–155304 (2002)
6. G.E. Volovik, JETP Lett. **75**, 418 (2002)
7. M.Y. Kagan, Sov. Phys. JETP **63**, 288 (1986)
8. J.L. Olsen, J. Low Temp. Phys. **61**(1/2), 17 (1985)
9. P.W. Egolf, J.L. Olsen, B. Roehricht, D.A. Weiss, Phys. B **169**, 217 (1991)
10. P.W. Egolf, D.A. Weiss, S.D. Nardo, J. Low Temp. Phys. **90**(3/4), 269 (1993)
11. L.V. Abdurahimov, A.A. Levchenko, L.P. Mezhov-Deglin, I.M. Khalatnikov, Low Temp. Phys. **38**(11), 1013 (2012)
12. R.J. Donnelly, C.F. Barenghi, J. Phys. Chem. Ref. Data **27**, 6 (1998)
13. I.M. Khalatnikov, J. Low Temp. Phys. **82**, 93 (1991)
14. I.M. Khalatnikov, G.V. Kolmakov, V.L. Pokrovskii, JETP **80**(5), 873 (1995)
15. I.M. Khalatnikov, M. Kroyter, J. Low Temp. Phys. **88**, 626 (1999)
16. MYu. Brazhnikov, A.A. Levchenko, L.P. Mezhov-Deglin, Instrum. Exp. Tech. **6**, 31 (2002)
17. L.V. Abdurahimov, MYu. Brazhnikov, A.A. Levchenko, A.M. Lihter, I.A. Remizov, Low Temp. Phys. **41**, 163 (2015)
18. AYu. Iznankin, L.P. Mezhov-Deglin, Sov. Phys. JETP **57**(4), 801 (1983)
19. V.B. Efimov, A.N. Ganshin, G.V. Kolmakov, P.V.E. McClintock, L.P. Mezhov-Deglin, Eur. Phys. J. Spec. Top. **185**, 181 (2010)
20. A. Makarov, J. Guo, S.W. Van Sciver, G.G. Ihas, D.N. McKinsey, W.F. Vinen, Phys. Rev. B **91**, 094503 (2015)
21. E.A. Kuznetsov, P.M. Lushnikov, JETP **81**(2), 332 (1995)
22. A.A. Levchenko, E. Teske, G.V. Kolmakov, P. Leiderer, L.P. Mezhov-Deglin, V.B. Shikin, JETP Lett. **65**(7), 572 (1997)